The Cryosphere Discuss., 7, 4545–4584, 2013
www.the-cryosphere-discuss.net/7/4545/2013/
doi:10.5194/tcd-7-4545-2013

The Cryosphere
Discussions
Open Access

Distribution and recent variations of supraglacial lakes on dendritic-type glaciers in the Khan Tengri-Tomur Mountains, Central Asia

Q. Liu[1], C. Mayer[2], and S. Liu[3]

[1]Key Laboratory of Mountain Surface Processes and Ecological Regulation, Institute of Mountain Hazards and Environment, Chinese Academy of Sciences, Chengdu, China
[2]Commission for Geodesy and Glaciology, Bavarian Academy of Sciences and Humanities, Munich, Germany
[3]Stake Key Laboratory of Cryospheric Sciences, Cold and Arid Regions Environmental and Engineering Research Institute, Chinese Academy of Sciences, Lanzhou, China

Received: 31 August 2013 – Accepted: 2 September 2013 – Published: 9 September 2013

Correspondence to: Q. Liu (liuqiao@imde.ac.cn)

Published by Copernicus Publications on behalf of the European Geosciences Union.

Abstract

Supraglacial lakes are widely distributed on glaciers in the Tomur-Khan Tengri Tianshan Mountains, Central Asia. The existence and development of supraglacial lakes play an important role in the ice melting processes and also in the storage and release of glacial melt water. Here we mapped the supraglacial lakes of eight typical debris-covered dendritic-type glaciers around the Tomur-Khan Tengri peaks based on 9 Landsat TM/ETM+ images acquired in the summers of 1990 until 2011. With a lower area limit of $3600\,m^2$ for a conservative identification of glacial lakes, we mapped 775 supraglacial lakes and 38 marginal glacial lakes in total. Our results indicate that supraglacial lakes (area $> 3600\,m^2$) in the study region never develop beyond an elevation of about 3850 m a.s.l., 800 m lower than the maximum upper boundary of debris cover (4650 m a.s.l.). The area-elevation distribution shows that lakes are predominantly occured close to the altitude of 3250 m a.s.l., where the clean ice simultaneously disappears. The majority of the supraglacial lakes are found on the Tomur Glacier and the South Inylchek Glacier, two strongly debris-covered dendritic-type glaciers in the region. As for the multi-year variation of lake area, the summer total and mean areas of supraglacial lakes show some variability from 1990 and 2005 but increased noticeably between 2005 and 2011. The mean area of the mapped lakes reached a maximum in 2010. We found that the area of supraglacial lakes is positively correlated to the total precipitation in summer (July to September) but negatively correlated to the mean spring air temperature (April to June). Pre-summer air temperature fluctuations likely have a stronger impact on the different evolution processes of glacial drainage, evolving from unconnected to connected systems, which may lead to the drainage of larger supraglacial lakes and results in shrinkage of the total and mean lake area during the summer.

1 Introduction

Glaciers act as natural water reservoirs because they store water as snow and ice in cold seasons and gradually release it by melting during the warm seasons. Variations of glacial runoff are primarily forced by the meteorological conditions, which alter the ice melt rate by changing the energy balance. Shorter time scales (diurnal or seasonal) changes of glacial runoff display periodic fluctuations and show more remarkable variations (Jansson et al., 2003) than that of longer time scales (interannual or decadal). Seasonal and diurnal glacial runoff reflects variations in atmospheric air temperatures and therefore the pattern of ablation on a glacier (Hock, 2005). In some cases this pattern of diurnal and seasonal discharge fluctuation is interrupted by catastrophic release events, such as glacial lake outburst floods (GLOFs) (Richardson and Reynolds, 2000) and subglacial floods (Jökulhlaups) (Roberts, 2005), etc. Such uncertainty of glacial melt water release results from the fact that glaciers act as "porous-medium" by storing liquid water and releasing it abruptly and stochastically through a changeable englacial and subglacial drainage system (Campbell and Rasmussen, 1973). Liquid water, supplied by melt or rainfall, can be stored in different kinds of water-accumulating features in a glacier, such as supraglacial lakes (ponds) and streams, crevasses, moulins, subglacial cavities (channels) and lakes, and different kinds of ice or moraine dammed lakes, etc (Fountain and Walder, 1998; Cuffey and Paterson, 2010). Much effort has been invested to study the evolution of glacier drainage systems using several methods, such as dye tracing experiments (Nienow et al., 1996; Schuler et al., 2004; Chandler et al., 2013), analyzing the chemical character of glacial melt water and runoff processes (Anderson et al., 2003), ground penetrating radar investigations (Kulessa et al., 2008), borehole observations (Fudge et al., 2008), etc. However, the location, amounts and release mechanisms of the stored water usually remains elusive due to its temporal and spatial variability (Fountain and Walder, 1998).

Among all components of a glacier drainage system, supraglacial ponds and lakes are the easiest to be detected. Although direct measurements of supraglacial ponds

TCD
7, 4545–4584, 2013

and lakes (Benn et al., 2000) are still limited, remote sensing observations have contributed to detect, measure and monitor their spatial and temporal changes in recent years (Wessels et al., 2002; Box and Ski, 2007; Gardelle et al., 2011; Salerno et al., 2012). Supraglacial lakes are commonly found in the lower ablation region of some debris-covered valley glaciers, where glacier ice stagnates (Reynolds, 2000; Benn et al., 2012). They are also formed, predominantly, in topographic lows and compressive flow regimes in the ablation zone of the Greenland Ice Sheet (Box and Ski, 2007; Bartholomew et al., 2011; Banwell et al., 2012). In the central Himalaya, their existence is found to enhance the ice ablation rate by ice margin calving processes around ponds and lakes (Sakai et al., 1998; Sakai et al., 2000; Benn et al., 2012). In particular, their total water volume and their water contribution to the overall water balance in a glacierised basin has never been evaluated, although this type of water storage could contain a significant amount of seasonally produced melt water (Fountain and Walder, 1998; Irvine-Fynn et al., 2011). Furthermore, their periodic (or seasonal) filling and drainage could impact the hydrological process of glacial runoff, and potentially influence glacier dynamics by enhancing subglacial lubrication and thus glacier sliding (Bingham et al., 2006; Das et al., 2008).

Supraglacial lakes are highly variable in space and time. Their lifetime is unpredictable and in situ monitoring is very limited (Benn et al., 2001). Most supraglacial lakes will be temporarily formed on the glacier surface when water accumulates in topographic lows, whereas the drainage can occur on any occasions. Many studies have highlighted the temporal evolution of glacial lakes in the central Himalaya and indicated that most of the current big moraine-dammed or ice-dammed lakes are the consequences of coalesce and growth of supraglacial lakes (Sakai et al., 2000; Komori, 2008; Fujita et al., 2009; Benn et al., 2012; Thompson et al., 2012). These glacial lakes pose a potential for GLOFs and destruction of property and loss of human life in the area downstream (Reynolds, 2000; Richardson and Reynolds, 2000; Bajracharya et al., 2007; Jain et al., 2012). Therefore, investigating the conditions of the supraglacial

TCD
7, 4545–4584, 2013

lakes (ponds) formation and distribution will be a significant contribution to tracing their dynamics and the prediction of their future development (Bolch et al., 2008).

In the central Tianshan region, supraglacial lakes are common on many debris-covered glaciers (Wang et al., 2011). The physical conditions of glaciers in the inner Tianshan region enable the formation of different types of glacial lakes. Moraine-dammed, ice-dammed, and supraglacial lakes are widely distributed on and adjacent to the glaciers. One of the largest moraine-dammed lakes is the Petrov Lake in the Ak-Shiirak massif, as reported by Jansky et al. (2009, 2010), which has experienced a dramatic increase in size during recent years. The probably most well-known ice-dammed lake, Lake Merzbacher, dammed by the South Inylchek Glacier, is famous for its regular outbursts at least once every summer that has lead to remarkable floods in the downstream valley (Mayer et al., 2008; Ng and Liu, 2009; Glazirin, 2010). However, the supraglacial lakes in this region were seldom considered in scientific investigations, even though they are widely distributed in the ablation zone (Han et al., 2010). Recently, several field observations were carried out to monitor some typical supraglacial lakes on the Koxkar Glacier (Wang et al., 2011). Here we investigated the supraglacial lakes on the large debris-covered glaciers of the Khan Tengri-Tomur Mountains in Central Asia based on mapping multi-year Landsat image series. The study focuses on the spatial distribution and temporal variations of these lakes from 1990 to 2011. A discussion will be emphasized about the formation conditions and consequences of the dynamics of these lakes.

2 Study area

The Tomur (Pobeda) Peak, 7439 m above sea level (a.s.l.), and the Khan Tengri Peak, 6995 m a.s.l., are the highest peaks of the Tianshan Mountains, located at the Kyrgyzstan-China border, southeast of Lake Issyk-Kul (Fig. 1). There are more than 40 peaks exceeding 6000 m a.s.l. in the Khan Tengri-Tomur Knot, which forms the largest glacierized complex in the Tianshan (Shi, 2008). A striking glaciological feature of this region is the existence of many large dendritic valley glaciers with thick debris covers. These glaciers are often classified as Tomur-type glaciers by Chinese glaciologists (Wang et al., 1980). The number of glaciers in this region adds up to 1375 (509 in China) with a total area of 4093 km^2 (Shi, 2008). Meltwater from these glaciers forms the major source for rivers in the internal drainage basins in Central Asia. Tarim river and Balkhash basin are the notable inland basins in which 45–50 % of the surface runoff is from glacial runoff (Aizen et al., 1997).

In the Khan Tengri-Tomur Mountains (KTTM), there are 7 glaciers larger than 100 km^2. An impressive characteristic of these glaciers is the extensive supraglacial debris mantle in their ablation zone (Han et al., 2006; Hagg et al., 2008). High amounts of solid precipitation in the firn basins and intensive melting in the ablation areas demonstrate that these glaciers have a high level of mass turnover (Aizen et al., 1997). High surface velocities at in the upper branches indicate a strong erosive and transport capacity (Mayer et al., 2008). Rock falls together with avalanches are probably the main the source of the supraglacial debris that is transported downwards by ice flow and finally forms the medial or lateral moraine belts on the surface of the ablation area of the glaciers (Aizen et al., 1997).

The KTTM region is located within the zone of the subtropical west jet stream in June to August, resulting in a summer precipitation maximum and cold and dry winters in this region. Data from the Tienshan station, to the West of this region, and KUQA weather station, on the eastern side (Fig. 1), show that 83 % (Tianshan station) to 79 % (KUQA station) of the annual precipitation falls in the months of April to September (Fig. 2). Precipitation at high altitude is significantly increased by orographic effects. Annual mean precipitation recorded at the Tianshan Station, 265 mm at 3639 m a.s.l., is about three to four fold higher than that recorded at the Kuqa Station, 74 mm at the 1100 m a.s.l. According to an ice core stratigraphic analysis from Inylchek Glacier in 1989, Aizen et al. (1997) reported an annual mean snow accumulation of 918 mm at 6148 m a.s.l. However, due to the lack of direct measurements of precipitation at elevations above 5000 m a.s.l., the validation for precipitation estimations at high elevations remains challenging.

3 Data and methods

Nine orthorectified Landsat TM or ETM+ images were used in this study to map the boundary of supraglacial lakes on eight selected glaciers (indicated in Fig. 1). The Landsat images, spanning the period from 1990 to 2011 with the same footprint, were selected and downloaded from the Landsat archive of the United State Geological Survey (USGS) based on the following criteria: (1) the lowermost part of the glaciers was (almost) cloud free or and not (or only minimal) covered by snow; (2) the image was acquired during the summer (July to September). The spatial resolution (pan-sharpen for Landsat ETM+ spectral bands) and acquisition date of these images are listed in Table 1.

The extent of the glaciers was manually adapted from the latest GLIMS dataset (Armstrong et al., 2012), based on a Landsat TM image acquired on 24 August 2007. After the glaciers outlines were delineated, clean ice and snow inside the boundary of glaciers was extracted from the image using a band ratio method, which applied a threshold algorithm on the Normalized Difference Snow Index (TM2 – TM5)/(TM2 + TM5). At the same time, the extent of debris-covered area of each glacier was also determined (Fig. 3).

To efficiently map supraglacial lakes, we first created a mask which includes all supraglacial lakes or marginal lakes (Figs. 3 and 4a). Outlines of the supraglacial lakes and marginal lakes were semi-automatically extracted from Landsat image in each year using the ENVI object-based Feature Extraction Module (IDL, 2008). Its workflow consists of two primary steps: find objects and extract features. By adjusting parameters for the scale level and merge level, the procedure is interactively performed to observe whether the lakes boundaries are well delineated or not (Fig. 4b). We used this procedure to generate polygon shape files, where the combination of segments finally occupies the whole masked region (Fig. 4c). These polygons were then overlaid on the source Landsat image and modified visually by keeping the polygons of lakes only and merge the connected polygons to one lake (Fig. 4d). For most Landsat images used, the spatial resolution is about 30 m which requires an area threshold of 3600 m^2 on the final mapping results for the analysis of the supraglacial lakes distribution and changes (Wessels et al., 2002; Gardelle et al., 2011). The uncertainty in the measurement of the lake area was estimated by assuming an error of ±0.5 pixel on the outlines of the shape (Fujita et al., 2009; Salerno et al., 2012).

In order to exploit the geomorphological characteristics of the glaciers and lakes, we also applied the Shuttle Radar Topography Mission (SRTM V4) digital elevation model (DEM) of 90 m horizontal resolution (http://srtm.csi.cgiar.org/) that has been void filled (Reuter et al., 2007; Jarvis et al., 2008) to demonstrate the hypsography of lakes and glaciers. Since changes of the glacier surface elevation were not remarkable in this region between 1999 and 2009 (-0.23 ± 0.19 m w.e. a^{-1}) (Pieczonka et al., 2013), we assume that, for the statistics on area-elevation distributions of glaciers and supraglacial lakes for each 100 m altitude zone, potential variations of the surface elevation could be neglected. We also ignored the accompanied uncertainty for the calculation of glacier surface gradients since the calculated surface gradient is based on the relative values between DEM pixels (Quincey et al., 2007) .

4 Results

4.1 Glaciers and supraglacial lakes distribution

The 8 selected glaciers, with a total area of 2101.8 km^2, account for about 51 % of the area of all glaciers (about 4093 km^2) in the KTTM region. They are spanning from 2689 m a.s.l. to 7053 m a.s.l. Debris cover in the lower part of these glaciers occupies about 17.2 % of the total glacier area. There exist general morphological features common to all glaciers. For example, the accumulation areas are always steep while the ablation areas are normally gentle when examining the surface slopes along their central flow lines (Fig. 3). On average, the slope of the upstream part of the glaciers is $\sim 42.1^{\circ}$ and that in the lower part is $\sim 8.9^{\circ}$. Both, the debris cover and the observed supraglacial lakes are located in the lower downstream part of the glaciers.

Since we observed that the majority of supraglacial lakes were located on the Tomur Glacier (TG) and the South Inylchek Glacier (SIG), the detailed statistical results of these two glaciers are presented here. The SIG is the largest glacier in the KTTM region, 607.13 km^2 in area and 53.7 km in length. Part of its lower branch is calving into the Merzbacher Lake, an ice dammed lake located between the south and north Inylchek Glaciers, with a maximum area of about 4 km^2. It is the origin of periodical outburst floods at least once every summer since the early 1900s (Mayer et al., 2008; Ng and Liu, 2009; Glazirin, 2010). The Merzbacher Lake will not be included in our discussion since its size is far out of the range of most supraglacial lakes investigated in this region and, actually, few Landsat images used here have ever captured the lake when it is filled. The statistics of all mapped supraglacial lakes (the Lake Merzbacher excluded) are presented in Table 2.

During 1990–2011, the summer 1990 shows the largest total area of supraglacial lakes while the summer 2005 shows the minimum. Total area of the supraglacial lakes on TG and SIG occupied from 43.9 % (in 1990) to 72.6 % (in 2005) of all mapped lakes in the KTTM region, with a slightly larger percentage in numbers from 50 to 74 %, respectively. Supraglacial lakes mapped in 1990 and 2005 are presented in Fig. 3, and their numbers and the total area grouped by individual glacier are listed in Table 2. The total number of supraglacial lakes plotted in Fig. 3 is 180, with 103 in the summer of 1990 and 77 in 2005.

Figure 5 displays the distribution of the supraglacial lakes area (as the mean value of all years) with elevation, compared to the area-altitude distribution of clean ice and debris for all eight glaciers and TG and SIG separately. For these glaciers, most of the clean ice surface occurs above 4000 m a.s.l. (90.1 %) and reaches its maximum at about 4750 m a.s.l. On the other hands, most the debris-covered area is distributed below 4000 m a.s.l. (89.1 %) and reaches its maximum at about 3750 m a.s.l. Supraglacial lakes can be found at a highest elevation of 3850 m a.s.l., which is about 800 m lower than the upper boundary of surface debris (4650 m a.s.l.). Supraglacial lakes reach their maximum total area at about 3250 m a.s.l. below which nearly no clean ice is observed. Therefore, these results indicate that, for the studied glaciers the debris cover appears in the region closest to the clean ice area maximum, while the supraglacial lakes appear in the region closest to the debris cover area maximum and the lake area reaches a maximum coinciding with the disappearance of clean ice.

4.2 Multi-year variations of supraglacial lakes

Few studies have systematically investigated the temporal variations of supraglacial lakes considering their total area in a mountain region or on a specific glacier (Gardelle et al., 2011; Salerno et al., 2012). Based on the lakes mapping results, the total and mean area of supraglacial lakes was computed for the TG, the SIG and the whole KTTM, for the summers 1990–2011 (Fig. 6). The images are all acquired with one and a half month of late summer, early autumn. Therefore they represent a general late summer condition of lake evolution. All the statistical data is listed in the Table 3. In general, the total area of supraglacial lakes on the TG is larger than the SIG. Over the study period, there was no general trend detected for either the total area or the mean area. In some specific years, however, the extent of supraglacial lakes showed more pronounced increases than in some other years. For the whole KTTM region, the total area of supraglacial lakes varied between $0.628 \pm 0.063\,km^2$ in 2005 and $1.400 \pm 0.224\,km^2$ in 1990, with a mean value of $0.918 \pm 0.149\,km^2$. Total area of supraglacial lakes in summer of 1990 was more than twofold larger than in 2005. Between 1990 and 2005, the total area of supraglacial lakes showed large fluctuations. In the more recent years, between 2005 and 2011, however, the total area of supraglacial lakes experienced an expanding trend. This trend is also seen on the TG and the SIG, although there existed several heterogeneous periods of expansion or shrinkage.

The variation of the annual mean area of supraglacial lakes is presented in Fig. 6b. Supraglacial lakes on the TG and the SIG generally expanded in this period, although the mean area shows a large variability. The mean area of all investigated supraglacial lakes varied between $0.007 \pm 0.001\,km^2$ (for the SIG in 2005) and $0.018 \pm 0.002\,km^2$ (for the TG in 2010). For both the KTTM region and the two glaciers, the averaged multi years mean area of supraglacial lakes is closed to the same value ($0.010 \pm 0.002\,km^2$, for the whole KTTM the value is $0.011 \pm 0.002\,km^2$, Table 3). The minimum mean area of supraglacial lakes in the KTTM region also occurred in 2005 ($0.008 \pm 0.001\,km^2$), while the maximum mean area occurred in 2010 and then in 1990. For the whole KTTM and the TG, the mean supraglacial lake area showed a transient maximum in 2010 after the gradual increase between 2005 and 2010 and then decreased again to the mean size of $0.009 \pm 0.002\,km^2$ in 2011. During the 9 yr period between 1990 and 2011, a total of 775 supraglacial lakes in the KTTM region were mapped, with an annual mean number of 86. The annual mean number of supraglacial lakes on the TG and SIG were 33 (38.4 %) and 23 (26.7 %), respectively. Since the mean lake size changed only on a moderate scale, the year-to-year fluctuation of the lake numbers is an important parameter to determine the total area variation. For example the growth of total area of supraglacial lakes in summer of 2011 displayed in Fig. 6a was governed by the increase of lake numbers.

For different area classes of supraglacial lakes, the number and total area also show different year-by-year variations (Fig. 7). The number of smaller supraglacial lakes (area $< 0.01\,km^2$) is by far larger than the bigger lakes (area $> 0.01\,km^2$). On the average between 1990 and 2011, the numbers of supraglacial lakes were 60, 17 and 9 for areas $< 0.01\,km^2$, between $0.01\,km^2$ and $0.02\,km^2$ and $> 0.02\,km^2$, respectively. The total area of supraglacial lakes for the 3 area classes, however, contributed nearly equally to the overall lakes area of the individual year, with mean values of $0.36\,km^2$, $0.23\,km^2$ and $0.32\,km^2$ for the different area classes. Generally, larger supraglacial lakes show more remarkable variations in area than smaller lakes. It is obvious that the anomalies

TCD
7, 4545–4584, 2013

of the total area which occurred in 1990, 2002 and 2005 were predominant due to the area changes of larger supraglacial lakes (Fig. 7, right panel).

5 Discussions

5.1 Glacio-geomorphological control on the supraglacial lake formation, expansion and drainage

All mapped supraglacial lakes in the KTTM region are detected in the lower flat downstream part of the investigated glaciers. Their locations and sizes show remarkable fluctuations year by year. This flatter part of the glaciers (with a mean slope of 8.9°) is also the region where extensive debris-cover exists in (Figs. 3 and 8). The formation and existence of supraglacial lakes is strongly related to the local surface slope (Sakai and Fujita, 2010). According to Reynolds (2000), at a surface gradient less than 10° supraglacial lakes can form and potentially exist for some duration. The formation of larger supraglacial lakes can occur where surface gradients range between 0–2°. In Fig. 9, we plotted all mapped 775 supraglacial lakes and 38 marginal lakes, classified into the 3 categories of lake size ($< 0.01\,km^2$, 0.01–$0.02\,km^2$ and $> 0.02\,km^2$), on the surface gradient map of the eight investigated glaciers. Following the classification by Reynolds (2000) and Bolch et al. (2008), glacier surface slope was divided into 5 classes based on the SRTM DEM. As mentioned by Bolch et al. (2008), lake areas in the elevation model also contain short steep slopes of ice cliffs around the supraglacial lakes or ponds. Therefore, to reduce the noise induced by ice cliffs, the slope relating to a supraglacial lake was calculated from the value of adjacent DEM cells nearby the center of the lake using bilinear interpolation. Figure 10 shows the calculated surface slopes plotted against the lakes area. It is obvious that most large lakes (71 of 86 lakes with area $> 0.02\,km^2$) are located in the region with surface gradients less than 10°. In the same way, for the 689 supraglacial lakes with an area less than $0.02\,km^2$, 608 of them are located in the region with surface gradient less then 10°.

Further statistics based on the slope classification for the total lake area (normalized to the annual mean value for the 9 yr) and numbers of supraglacial lakes are presented in the right two panels of Fig. 10. As it's expected, both the total area and the numbers of supraglacial lakes show a decrease with increasing surface slope. The annual mean total area of supraglacial lakes located in regions of less than 10° surface gradient accounts for 85.7 % of the total. The statistic based on the classification suggested by Reynolds (2000), however, indicates that large portion of lake area in the KTTM is distributed in the regions with surface gradient between 2 and 6° but not the value less than 2° suggested by Reynolds (2000). This similar fact could also be detected in the Figure 5 in Bolch et al. (2008). These could be explained by the frequency distribution of surface slope of the entire debris-covered area (Fig. 10d). Since the area of surface gradient between 2° and 6° accounts for the majority portion (42.8 %) in the lower ablation zone of these glaciers and it is also very favorable for the development of supraglacial lakes, lake area reaching its maximum in these regions is naturally.

Once a supraglacial lake forms, it will grow rapidly due to several coupled physical mechanisms leading to enhanced ice melt around and on the subaqueous interface of the lake (Benn et al., 2000; Reynolds, 2000; Benn et al., 2001). Generally, sources of lake water include (1) melting of ice around the lake and within the lake itself, (2) melt water transported through englacial channels or inflow from supraglacial streams and (3) water directly supplied by rainfall or snow melt. On the debris-covered glaciers in the KTTM region, the widespread ice cliffs are characterized by higher ablation rate than its surrounding debris covered ice and even higher than on the flat clean ice surface (Han et al., 2010; Mayer et al., 2011). In addition to the liquid water directly supplied by precipitation, melting from ice cliffs around a supraglacial lake contributes the main accumulated water for the lake formation and growth (Benn et al., 2001). On the Koxkar Glacier, Han et al. (2010) reported that about 1.13 % (0.22 km^2) of the total debris-covered area was occupied by the ice cliffs and melting from ice cliffs produces about 7.3 % (1.6×10^6 km^3) of the total melt runoff from the debris-covered area. As an ice cliff melts back, surface debris and rocks falling into the water will also raise the

TCD
7, 4545–4584, 2013

lake level. Together with the process of water-line melting (Benn et al., 2001), these will all contribute to the lake growth (Fig. 11).

On the other hand, the growth of a supraglacial lake will be balanced by a combination of lake water loss via outflow and evaporation. Continuous lateral calving and melt at the water-line and subsurface down-cutting may lead to abrupt drainage of the lake, when encountering an ice crevasse or englacial channels (Fountain and Walder, 1998; Irvine-Fynn et al., 2011). Repeated observations of supraglacial lakes on the Ngozumpa Glacier in the Khumbu Himalaya (Benn et al., 2001) and also on the Koxkar Glacier during our 2010 expedition (Fig. 12) indicate the existence of connections between supraglacial lakes and glacial drainage systems before the lake drainage. Sometimes the activation of this connection is due to ice motions, which may open a pathway for lake water drainage (van der Veen, 2007; Das et al., 2008).

We did not extract the surface velocity of investigated glaciers, although the flow velocity of a glacier is inherently related to its surface slope (Paterson, 1994). Further investigations are needed for depicting the region-wide spatial distribution pattern of glacier surface velocity fields, which may play a more direct role in controlling the existence and lifespan of a supraglacial lake (Bolch et al., 2008; Benn et al., 2012). Surface flow fields of individual glaciers may help to illustrate the possible reasons for the infrequent existence of supraglacial lakes on the surface of some glaciers, such as the Muzart Glacier (given the similar patterns of debris-cover, surface gradients and relative lower ice tongue); and analyzing multi-year changes of velocity may also contribute to the explanation of the supraglacial lake's year-to-year fluctuations.

Based on the currently available satellite products, it is difficult to detect seasonal variations of supraglacial lakes in the KTTM region (in colder seasons mapping is usually influenced by snow cover, lake ice or cloud). For supraglacial lakes on the Greenland Ice Sheet, due to their relative larger sizes (diameter ranges from a few hundred meters to >2 km) (Box and Ski, 2007), their seasonal variation could be detected by repeat middle-resolution satellite images (McMillan et al., 2007; Sundal et al., 2009; Johansson et al., 2013). For mountain valley glaciers, however, supraglacial lakes are generally too small (also unstable) to be repeatedly observed by middle-resolution satellites. Therefore, the current study concentrated the multi-year variations of supraglacial lakes for late summer conditions.

In the KTTM region, no moraine dammed glacial lake was found until present time, in contrast to the large number detected on debris-covered glaciers in the Himalaya (Richardson and Reynolds, 2000; Komori, 2008), the southern Alps (Kirkbride and Warren, 1999; Warren and Kirkbride, 2003) and the Patagonian Andes (Reynolds, 1992; Dussaillant et al., 2009). It has been confirmed that most of these reported moraine dammed lakes are a result of the expanding and merging of supraglacial lakes that periodically fill up on the surface of extensive debris-covered parts of glaciers (Reynolds, 2000). In the lower part of the dendritic-type glaciers in the KTTM, we have identified some regions where supraglacial lakes are likely to develop (Fig. 8). These regions are prone to coalesce and growth of supraglacial lakes, lending the potential for larger lake development. Actually, from results of the current investigation, most supraglacial lakes with an area larger than 0.02 km^2 are also located in the same regions. Regarding water storage, flood hazards and also the influence of lakes on the glacier characteristics and dynamics, these water bodies with larger areas are much more important than the small ones.

5.2 Relationship between supraglacial lakes variation and climatic conditions in summer and spring

As previously mentioned, supraglacial lakes are highly variable in space and time. The size of supraglacial lakes varies with the lake water balance. During winter time, lakes either disappear (due to the lack of water input), or freeze over. Ignoring the glacial surface topographic changes, the lake evolution will be primarily affected by the climatic variations. Considering that the state of supraglacial lakes in summer are influenced by both summer and pre-summer conditions, we therefore extracted total precipitation and mean air temperature over summer (July to September) and spring (April to June) for each specific year from monthly climatic data of the Tianshan Station (Fig. 13).

Between 1990 and 2011, the variation of total precipitation over the two seasons is remarkable. For example precipitation over the ablation season in 1990 was peculiarly higher (about 5 times) than in 2005 or 2006. For air temperature, its summer mean values show less fluctuation than during spring, which dominate the multi-year variations of mean air temperature for the whole ablation season between 1990 and 2011.

By comparing the climatic fluctuations (Fig. 13) with the variations of supraglacial lakes (Fig. 6), we found that the area of supraglacial lakes was positively correlated with precipitation, while correlation was negative with respect to the mean air temperature. Since liquid precipitation acts as the direct input of liquid water into the supraglacial lakes, its total amount over summer is positively correlated to the area of supraglacial lakes. Air temperature increase, however, has a dual function in the development of supraglacial lakes: more melt water enlarges the supraglacial lakes due to enhanced ablation and, on the other hand, it may accelerate the drainage of lakes by promoting the development of glacial drainage systems from unconnected to connected structures (Irvine-Fynn et al., 2011). In some years, such as in 1990, the drainage of supraglacial lakes is likely to be limited by the relatively cool ablation season whereas a superimposed precipitation (if snow then it will melt soon during the ablation season) contributes water input to the lake expansions. In 2005, in contrast, little precipitation (especially over summer) together with a warmer ablation season could explain the observations of the minimum total and mean area of supraglacial lakes in that summer.

From Figure 14, the relationships between the lake area and climatic conditions can be recognized. An obviously negative correlation between supraglacial lakes area and mean air temperature for spring (April to June) but not for summer (July to September) likely indicates that most connected drainage systems have been developed between April and June. The development of glacial drainage systems leads to some drainage of supraglacial lakes, resulting in the lakes total area shrinkage. The mean area of supraglacial lakes also decreased with the increase of mean air temperature during spring. This likely indicates that more drainage events happened to larger supraglacial lakes, which could have induced a general decrease of mean lake area. This could also be confirmed by Fig. 7 that, in the summer of 2005, the remarkable shrinkage (both the numbers and their total area) of larger supraglacial lakes contributed to the major variations, whereas no remarkable changes happened to the smaller lakes.

6 Conclusions

We presented the distribution and multi-year variations of supraglacial lakes for several selected glaciers around the KTTM region, the largest glacierized mountain range in the Tianshan. A total of 775 supraglacial lakes and 38 marginal glacial lakes (minimum size 3600 m^2) were mapped on Landsat images in the period 1990 to 2011. This relates to a mean of 86 lakes occurring each year on these glaciers. The distribution of all mapped supraglacial lakes shows that supraglacial lakes in the KTTM region initially appear at about 3850 m a.s.l., about 800 m lower than the debris cover emergence (4650 m a.s.l.), and reach their maximum area at about 3250 m a.s.l., the altitude where bare ice disappears entirely. For the whole KTTM region, the total area of supraglacial lakes varied between 0.628 ± 0.063 km^2 in 2005 and 1.400 ± 0.224 km^2 in 1990, with a mean value of 0.918 ± 0.149 km^2. The total area of supraglacial lakes showed large fluctuations between 1990 and 2005 whereas in recent years, between 2005 and 2011, experienced an expanding trend. Mean area of supraglacial lakes showed a transient maximum in 2010 after the expanding between 2005 and 2010 and then decreased to the mean size scale of 0.009 ± 0.002 km^2 in 2011. The area of supraglacial lakes was positively correlated with the total precipitation in summer (July to September) while correlated negatively to the mean air temperature over pre-summer (April to June). Air temperature fluctuations during the pre-summer likely have more impact on the different evolution proceedings of the development of glacial drainage from unconnected to connected systems, which may lead to the drainage of some larger supraglacial lakes and resulted in shrinkage of the total and mean lakes area over the summer seasons.

The majority of the investigated supraglacial lakes were located on the surface of the Tomur Glacier and the South Inylchek Glacier, two typical debris-covered dendritic-type glaciers in the KTTM region. The total area of supraglacial lakes on the surface of TG and SIG occupied 43.9 % (in 1990) to 72.6 % (in 2005) of all mapped lakes in the KTTM regions, and accounted for 50 % to 74 % in numbers, respectively. Some regions in the lower part of the TG and SIG are found more favorable for the supraglacial lakes development. Future coalescing and growth of these supraglacial lakes will lead to the development of larger lake on lower part of the glaciers. A continued monitoring is necessary to assess the future evolution of supraglacial lakes in the KTTM region.

Acknowledgements. Our work was initiated from the Chinese-German collaborative field expedition at the Koxkar Glacier in the Tomur Mountains, partly funded by the Deutsche Forschungsgemeinschaft (DFG fund MA 3347/4). Thanks to Han Haidong, Wang Xin, Martin June and Elisabeth Mayr for the field assistance. This work was funded by the National Science and Technology Support Program of Chinese MOST (Grant No. 2012BAC19B07 and 2013BAC10B01), the National Natural Science Foundation of China (Grant No. 41190080, 41371094) and a DAAD research-stay funding award (A-12-00042). The work was also supported by the Fund of State Key Laboratory of Cryosphere Sciences (Grant No. SKLCS 2011-10).

References

Aizen, V. B., Aizen, E. M., Dozier, J., Melack, J. M., Sexton, D. D., and Nesterov, V. N.: Glacial regime of the highest Tien Shan mountain, Pobeda-Khan Tengry massif, J. Glaciol., 43, 503–512, 1997.

Anderson, S. P., Longacre, S. A., and Kraal, E. R.: Patterns of water chemistry and discharge in the glacier-fed Kennicott River, Alaska: evidence for subglacial water storage cycles, Chem. Geol., 202, 297–312, doi:10.1016/j.chemgeo.2003.01.001, 2003.

Armstrong, R., Raup, B., Khalsa, S. J. S., Barry, R., Kargel, J., Helm, C., and Kieffer, H.: GLIMS glacier database, National Snow and Ice Data Center, Digital media, Boulder, Colorado USA, 2012.

Bajracharya, B., Shrestha, A. B., and Rajbhandari, L.: Glacial lake outburst floods in the Sagarmatha region – Hazard assessment using GIS and hydrodynamic modeling, Mt. Res. Dev., 27, 336–344, doi:10.1659/mrd.0783, 2007.

Banwell, A. F., Arnold, N. S., Willis, I. C., Tedesco, M., and Ahlstrøm, A. P.: Modeling supraglacial water routing and lake filling on the Greenland Ice Sheet, J. Geophys. Res., 117, F04012, doi:10.1029/2012JF002393, 2012.

Bartholomew, I., Nienow, P., Sole, A., Mair, D., Cowton, T., Palmer, S., and Wadham, J.: Supraglacial forcing of subglacial drainage in the ablation zone of the Greenland ice sheet, J. Geophys. Res., 38, L08502, doi:10.1029/2011GL047063, 2011.

Benn, D., Benn, T., Hands, K., Gulley, J., Luckman, A., Nicholson, L., Quincey, D., Thompson, S., Toumi, R., and Wiseman, S.: Response of debris-covered glaciers in the Mount Everest region to recent warming, and implications for outburst flood hazards, Earth-Sci. Rev., 114, 156–174, 2012.

Benn, D. I., Wiseman, S., and Hands, K. A.: Growth and drainage of supraglacial lakes on debris-mantled Ngozumpa Glacier, Khumbu Himal, Nepal, J. Glaciol., 47, 626–638, 2001.

Benn, D. I., Wiseman, S., and Warren, C. R.: Rapid growth of a supraglacial lake, Ngozumpa Glacier, Khumbu Himal, Nepal, IAHS-AISH P., 264, 177–185, 2000.

Bingham, R. G., Nienow, P. W., Sharp, M. J., and Copland, L.: Hydrology and dynamics of a polythermal (mostly cold) High Arctic glacier, Earth Surf. Proc. Land., 31, 1463–1479, doi:10.1002/esp.1374, 2006.

Bolch, T., Buchroithner, M. F., Peters, J., Baessler, M., and Bajracharya, S.: Identification of glacier motion and potentially dangerous glacial lakes in the Mt. Everest region/Nepal using spaceborne imagery, Nat. Hazards Earth Syst. Sci., 8, 1329–1340, doi:10.5194/nhess-8-1329-2008, 2008.

Box, J. E. and Ski, K.: Remote sounding of Greenland supraglacial melt lakes: implications for subglacial hydraulics, J. Glaciol., 53, 257–265, 2007.

Campbell, W. J. and Rasmussen, L. A.: The production, flow and distribution of melt water in a glacier treated as a porous medium, Hydrology of Glaciers, 11–27, 1973.

Chandler, D. M., Wadham, J. L., Lis, G. P., Cowton, T., Sole, A., Bartholomew, I., Telling, J., Nienow, P., Bagshaw, E. B., Mair, D., Vinen, S., and Hubbard, A.: Evolution of the subglacial drainage system beneath the Greenland Ice Sheet revealed by tracers, Nat. Geosci., 6, 195–198, doi:10.1038/Ngeo1737, 2013.

Cuffey, K. M. and Paterson, W. S. B.: The Physics of Glaciers, 4th Edition, Elsevier, 2010.

Das, S. B., Joughin, I., Behn, M. D., Howat, I. M., King, M. A., Lizarralde, D., and Bhatia, M. P.: Fracture propagation to the base of the Greenland Ice Sheet during supraglacial lake drainage, Science, 320, 778–781, doi:10.1126/science.1153360, 2008.
Dussaillant, A., Benito, G., Buytaert, W., Carling, P., Meier, C., and Espinoza, F.: Repeated glacial-lake outburst ?oods in Patagonia: an increasing hazard?, Nat. Hazards, 54, 469–481, doi:10.1007/s11069-009-9479-8, 2009.
Fountain, A. G., and Walder, J. S.: Water flow through temperate glaciers, Rev. Geophys., 36, 299–328, 1998.
Fudge, T. J., Humphrey, N. F., Harper, J. T., and Pfeffer, W. T.: Diurnal fluctuations in borehole water levels: configuration of the drainage system beneath Bench Glacier, Alaska, USA, J. Glaciol., 54, 297–306, 2008.
Fujita, K., Sakai, A., Nuimura, T., Yamaguchi, S., and Sharma, R. R.: Recent changes in Imja Glacial Lake and its damming moraine in the Nepal Himalaya revealed by in situ surveys and multi-temporal ASTER imagery, Environ. Res. Lett., 4, 045205, doi:10.1088/1748-9326/4/4/045205, 2009.
Gardelle, J., Arnaud, Y., and Berthier, E.: Contrasted evolution of glacial lakes along the Hindu Kush Himalaya mountain range between 1990 and 2009, Global Planet. Change, 75, 47–55, doi:10.1016/j.gloplacha.2010.10.003, 2011.
Glazirin, G. E.: A century of investigations on outbursts of the ice-dammed lake Merzbacher (central Tien Shan), Aust. J. Earth Sci., 103, 171–179, 2010.
Hagg, W., Mayer, C., Lambrecht, A., and Helm, A.: Sub-debris melt rates on southern Inylchek Glacier, central Tian Shan, Geogr. Ann. A, 90, 55–63, 2008.
Han, H., Jian, W., Junfeng, W., and Shiyin, L.: Backwasting rate on debris-covered Koxkar glacier, Tuomuer mountain, China, J. Glaciol., 56, 287–296, 2010.
Han, H. D., Ding, Y. J., and Liu, S. Y.: A simple model to estimate ice ablation under a thick debris layer, J. Glaciol., 52, 528–536, 2006.
Hock, R.: Glacier melt: a review of processes and their modelling, Progr. Phys. Geogr., 29, 362–391, doi:10.1191/0309133305pp453ra, 2005.
ENVI Feature Extraction Module User's Guide, 2008.
Irvine-Fynn, T. D. L., Hodson, A. J., Moorman, B. J., Vatne, G., and Hubbard, A. L.: Polythermal glacier hydrology: a review, Rev. Geophys., 49, RG4002, doi:10.1029/2010RG000350, 2011.

Jain, S. K., Lohani, A. K., Singh, R. D., Chaudhary, A., and Thakural, L. N.: Glacial lakes and glacial lake outburst flood in a Himalayan basin using remote sending and GIS, Nat. Hazards, 62, 887–899, doi:10.1007/s11069-012-0120-x, 2012.

Jansky, B., Engel, Z., Sobr, M., Benes, V., Spacek, K., and Yerokhin, S.: The evolution of Petrov lake and moraine dam rupture risk (Tien-Shan, Kyrgyzstan), Nat. Hazards, 50, 83–96, doi:10.1007/s11069-008-9321-8, 2009.

Jansky, B., Sobr, M., and Engel, Z.: Outburst flood hazard: case studies from the Tien-Shan Mountains, Kyrgyzstan, Limnologica, 40, 358–364, 2010.

Jansson, P., Hock, R., and Schneider, T.: The concept of glacier storage: a review, J. Hydrol., 282 116–129, 2003.

Jarvis, A., Reuter, H. I., Nelson, A., and Guevara, E.: Hole-filled seamless SRTM data V4, International Centre for Tropical Agriculture (CIAT), available at: http://srtm.csi.cgiar.org, 2008.

Johansson, A. M., Jansson, P., and Brown, I. A.: Spatial and temporal variations in lakes on the Greenland Ice Sheet, J. Hydrol., 476, 314–320, 2013.

Kirkbride, M. P. and Warren, C. R.: Tasman Glacier, New Zealand: 20th-century thinning and predicted calving retreat, Global Planet. Change, 22, 11–28, 1999.

Komori, J.: Recent expansions of glacial lakes in the Bhutan Himalayas, Quatern. Int., 184, 177–186, 2008.

Kulessa, B., Booth, A. D., Hobbs, A., and Hubbard, A. L.: Automated monitoring of subglacial hydrological processes with ground-penetrating radar (GPR) at high temporal resolution: scope and potential pitfalls, Geophys. Res. Lett., 35, L24502, doi:10.1029/2008gl035855, 2008.

Mayer, C., Lambrecht, A., Eder, K., Juen, M., and Liu, Q.: Ice cliff ablation derived from high resolution surface models, based on close-range photogrammetry, Geophys. Res. Abstr., 13, EGU2011-11078, 2011.

Mayer, C., Lambrecht, A., Hagg, W., Helm, A., and Scharrer, K.: Post-drainage ice dam response at Lake Merzbacher, Inylchek glacier, Kyrgyzstan, Geogr. Ann. A, 90, 87–96, 2008.

McMillan, M., Nienow, P., Shepherd, A., Benham, T., and Sole, A.: Seasonal evolution of supra-glacial lakes on the Greenland Ice Sheet, Earth Planet. Sci. Lett., 262, 484–492, doi:10.1016/j.epsl.2007.08.002, 2007.

Ng, F. and Liu, S. Y.: Temporal dynamics of a jökkulhlaup system, J. Glaciol., 55, 651–665, 2009.

Nienow, P., Sharp, M., and Willis, I.: Temporal switching between englacial and subglacial drainage pathways: Dye tracer evidence from the Haut Glacier d'Arolla, Switzerland, Geogr. Ann. A, 78, 51–60, 1996.

Paterson, W.: The physics of glaciers (3rd Edn.), Oxford Press, Butterworth-Heinemann, 1994.

Pieczonka, T., Bolch, T., Junfeng, W., and Shiyin, L.: Heterogeneous mass loss of glaciers in the Aksu-Tarim Catchment (Central Tien Shan) revealed by 1976 KH-9 Hexagon and 2009 SPOT-5 stereo imagery, Remote Sens. Environ., 130, 233–244, 2013.

Quincey, D. J., Richardson, S. D., Luckman, A., Lucas, R. M., Reynolds, J. M., Hambrey, M. J., and Glasser, N. F.: Early recognition of glacial lake hazards in the Himalaya using remote sensing datasets, Global Planet. Change, 56, 137–152, doi:10.1016/j.gloplacha.2006.07.013, 2007.

Reuter, H. I., Nelson, A., and Jarvis, A.: An evaluation of void-filling interpolation methods for SRTM data, Int. J. Geogr. Inf. Sci., 21, 983–1008, 2007.

Reynolds, J.: The identification and mitigation of glacier-related hazards: examples from the Cordillera Blanca, Peru, in Geohazards, edited by: McCall, G. J. H., Laming, D. J. C., and Scott, S. C., Springer, 143–157, doi:10.1007/978-94-009-0381-4_13, 1992.

Reynolds, J. M.: On the formation of supraglacial lakes on debris-covered glaciers, IAHS Publication, 153–164, 2000.

Richardson, S. D. and Reynolds, J. M.: An overview of glacial hazards in the Himalayas, Quatern. Int., 65–66, 31–47, 2000.

Roberts, M. J.: Jökulhlaups: a reassessment of floodwater flow through glaciers, Rev. Geophys., 43, RG1002, doi:10.1029/2003RG000147, 2005.

Sakai, A. and Fujita, K.: Formation conditions of supraglacial lakes on debris-covered glaciers in the Himalaya, J. Glaciol., 56, 177–181, 2010.

Sakai, A., Nakawo, M., and Fujita, K.: Melt rate of ice cliffs on the Lirung Glacier, Nepal Himalayas, 1996, Bull. Glacier Res., 16, 57–66, 1998.

Sakai, A., Takeuchi, N., Fujita, K., and Nakawo, M.: Role of supraglacial ponds in the ablation process of a debris-covered glacier in the Nepal Himalayas, IAHS-AISH P., 265, 119–130, 2000.

Salerno, F., Thakuri, S., Agata, C. D., Smiraglia, C., Manfredi, E. C., Viviano, G., and Tartari, G.: Glacial lake distribution in the Mount Everest region: Uncertainty of measurement and conditions of formation, Global Planet. Change, 92–93, 30–39, doi:10.1016/j.gloplacha.2012.04.001, 2012.

Schuler, T., Fischer, U. H., and Gudmundsson, G. H.: Diurnal variability of subglacial drainage conditions as revealed by tracer experiments, J. Geophys. Res., 109, F02008, doi:10.1029/2003JF000082, 2004.

Shi, Y.: Concise glacier inventory of China, Shanghai, Shanghai Popular Science Press, 205 pp., 2008.

Sundal, A. V., Shepherd, A., Nienow, P., Hanna, E., Palmer, S., and Huybrechts, P.: Evolution of supra-glacial lakes across the Greenland Ice Sheet, Remote Sens. Environ., 113, 2164–2171, doi:10.1016/j.rse.2009.05.018, 2009.

Thompson, S. S., Benn, D. I., Dennis, K., and Luckman, A.: A rapidly growing moraine-dammed glacial lake on Ngozumpa Glacier, Nepal, Geomorphology, 145–146, 1–11, 2012.

van der Veen, C. J.: Fracture propagation as means of rapidly transferring surface meltwater to the base of glaciers, Geophys. Res. Lett., 34, L01501, doi:10.1029/2006gl028385, 2007.

Wang, L., Wenjing, Z., and Zhen, S.: Primary results of the study on modern glaciers in the region of Mt. Tuomuer, J. Glaciol. Geocryol., 2, 15–18, 1980 (in Chinese with English abstract).

Wang, X., Shiyin, L., Haidong, H., Jian, W., and Qiao, L.: Thermal regime of a supraglacial lake on the debris-covered Koxkar Glacier, southwest Tianshan, China, Environ. Earth Sci., 37, 175–183, doi:10.1007/s12665-011-1490-1, 2011.

Warren, C. R. and Kirkbride, M. P.: Calving speed and climatic sensitivity of New Zealand lake-calving glaciers, Ann. Glaciol., 36, 173–178, 2003.

Wessels, R. L., Kargel, J. S., and Kieffer, H. H.: ASTER measurement of supraglacial lakes in the Mount Everest region of the Himalaya, Ann. Glaciol., 34, 399–408, doi:10.3189/172756402781817545, 2002.

Table 1. List of Landsat images used in this study.

Image ID (File name)	Sensors	Spatial Resolution (m)	Acquisition Date (yyyy-mm-dd)
ETP147r31_5t19900910	TM	28.5	1990-09-10
LE71470311999238SGS00	ETM+	15	1999-08-26
LE71470312002230SGS00	ETM+	15	2002-08-18
LE71470312005222PFS00	ETM+	15	2005-08-10
LT51470312006249IKR00	TM	30	2006-09-06
LT51470312007236IKR00	TM	30	2007-08-24
LT51470312009273IKR01	TM	30	2009-09-30
LT51470312010228IKR01	TM	30	2010-08-16
LT51470312011231KHC01	TM	30	2011-08-19

TCD
7, 4545–4584, 2013

Table 2. Geomorphological characteristics of the eight selected glaciers, their debris-covered region and the 1990's and 2005's supraglacial lakes.

Glacier name	Glacier			Debris			Supraglacial lake in 1990		Supraglacial lake in 2005	
	Area (km^2)	Length (km)	Elevations (m a.s.l.)	Area (km^2)	Percentage (%)	Elevations (m a.s.l.)	Count	Total Area (km^2)	Count	Total Area (km^2)
Tomor Glacier	419.3	36.3	2754–6979	73.7	17.6	2754–4732	31	0.396 ± 0.031	40	0.328 ± 0.031
South Inylcheck Glacier	607.1	53.7	2895–7053	85.4	14.1	2895–4697	21	0.175 ± 0.016	17	0.115 ± 0.012
Kandy Glacier	118.7	25.5	3231–5654	16.0	13.5	3231–4130	7	0.069 ± 0.006	3	0.017 ± 0.002
Koxkar Glacier	86.9	25.6	3016–6037	21.4	24.6	3016–4244	6	0.128 ± 0.008	1	0.008 ± 0.001
Qong Terang Glacier	171.6	21.3	3026–7009	41.7	24.3	3026–4783	8	0.067 ± 0.006	6	0.052 ± 0.005
Tugaibieliqi Glacier	315.4	30.3	2689–6794	44.7	14.2	2689–5110	22	0.333 ± 0.025	8	0.074 ± 0.007
Hargol Glacier	211.4	32.2	2774–6457	37.3	17.6	2774–4923	8	0.131 ± 0.009	2	0.016 ± 0.002
Muzart Glacier	165.8	29.2	2763–6289	22.4	13.5	2763–4345	–	–	–	–
Total	2101.8	–	2689–7053	342.6	17.2	2689–5110	103	1.299 ± 0.103	77	0.610 ± 0.059

TCD
7, 4545–4584, 2013

Distribution and recent variations of supraglacial lakes

Q. Liu et al.

Table 3. Total and mean area of the supraglacial lakes during the investigated period.

Image Date	Pixel Size	Lakes of the Tomur Glacier			Lakes of the South Inylchek Glacier			Lakes of the whole KTTM Glacier		
	(m)	Total Area	Mean Area	Count	Total Area	Mean Area	Count	Total Area	Mean Area	Count
1990-9-10	28.5	0.396 ± 0.063	0.013 ± 0.002	31	0.176 ± 0.033	0.008 ± 0.002	21	1.400 ± 0.224	0.013 ± 0.002	112
1999-8-26	15	0.195 ± 0.019	0.009 ± 0.001	21	0.217 ± 0.019	0.011 ± 0.001	19	0.657 ± 0.058	0.011 ± 0.001	59
2002-8-18	15	0.244 ± 0.023	0.010 ± 0.001	25	0.296 ± 0.025	0.012 ± 0.001	25	1.066 ± 0.094	0.011 ± 0.001	96
2005-8-10	15	0.328 ± 0.033	0.008 ± 0.001	40	0.115 ± 0.012	0.007 ± 0.001	17	0.628 ± 0.063	0.008 ± 0.001	78
2006-9-06	30	0.311 ± 0.061	0.009 ± 0.002	36	0.257 ± 0.044	0.012 ± 0.002	22	0.770 ± 0.142	0.010 ± 0.002	77
2007-8-24	30	0.289 ± 0.055	0.009 ± 0.002	31	0.248 ± 0.047	0.010 ± 0.002	26	0.918 ± 0.169	0.010 ± 0.002	91
2009-9-30	30	0.406 ± 0.077	0.009 ± 0.002	44	0.162 ± 0.029	0.011 ± 0.002	15	0.883 ± 0.158	0.011 ± 0.002	82
2010-8-16	30	0.355 ± 0.052	0.018 ± 0.003	20	0.239 ± 0.044	0.010 ± 0.002	24	0.888 ± 0.144	0.014 ± 0.002	65
2011-8-19	30	0.405 ± 0.079	0.009 ± 0.002	46	0.322 ± 0.061	0.010 ± 0.002	35	1.054 ± 0.201	0.009 ± 0.002	115
Mean	–	0.322 ± 0.051	0.010 ± 0.002	33	0.234 ± 0.038	0.010 ± 0.002	23	0.918 ± 0.149	0.011 ± 0.002	86

TCD
7, 4545–4584, 2013

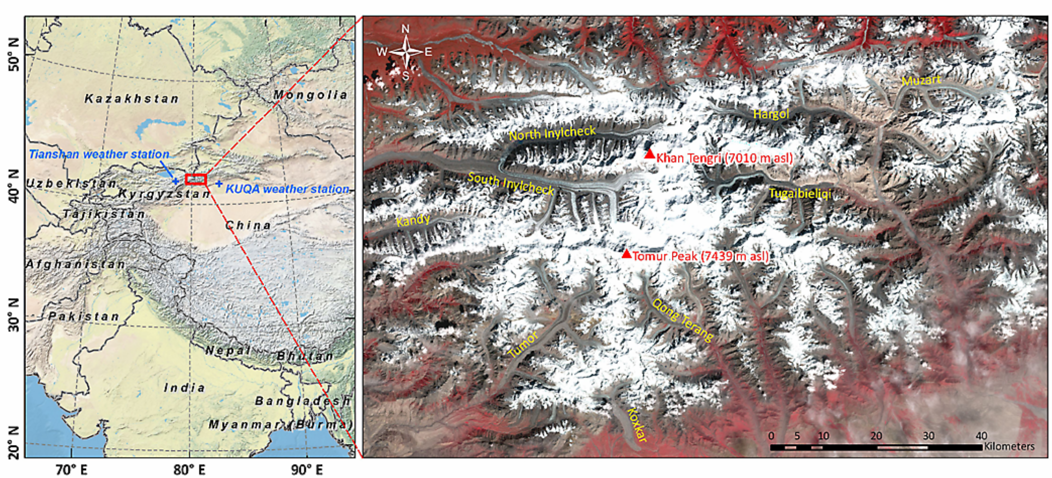

Fig. 1. Location map of the Khan Tengri-Tomur Mountains (left) and a Landsat TM image acquired on 24 August 2007 showing the distribution of main glaciers mentioned in the text (right).

TCD
7, 4545–4584, 2013

Distribution and recent variations of supraglacial lakes

Q. Liu et al.

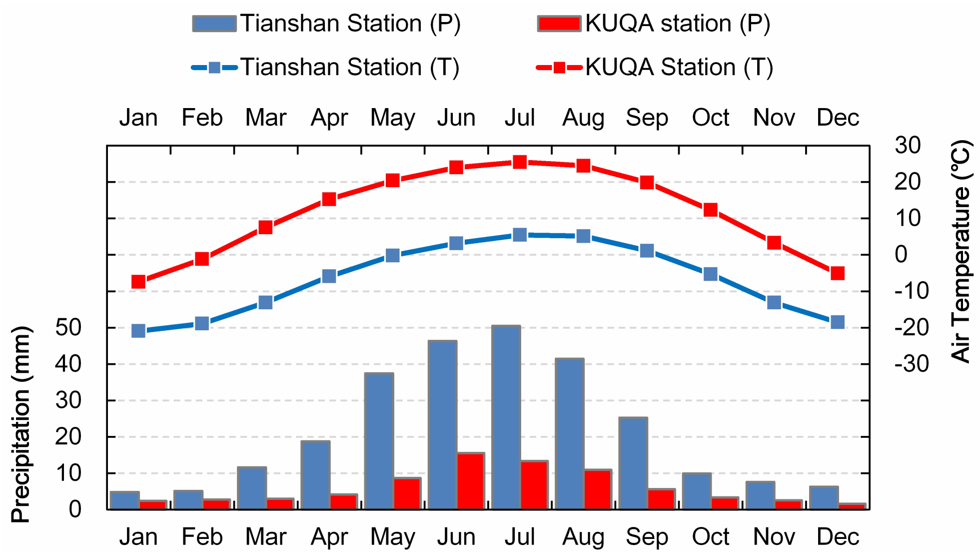

Fig. 2. Monthly mean air temperature (T) and precipitation (P) based on observations at the Tianshan weather station (3639 m, 1930–2011) and KUQA weather station (1100 m, 1951–2011).

TCD
7, 4545–4584, 2013

Distribution and recent variations of supraglacial lakes

Q. Liu et al.

Title Page
Abstract Introduction
Conclusions References
Tables Figures
◀ ▶
Back Close
Full Screen / Esc
Printer-friendly Version
Interactive Discussion

TCD
7, 4545–4584, 2013

Distribution and recent variations of supraglacial lakes

Q. Liu et al.

Title Page
Abstract
Introduction
Conclusions
References
Tables
Figures
◀◀ ▶▶
◀ ▶
Back
Close
Full Screen / Esc
Printer-friendly Version
Interactive Discussion

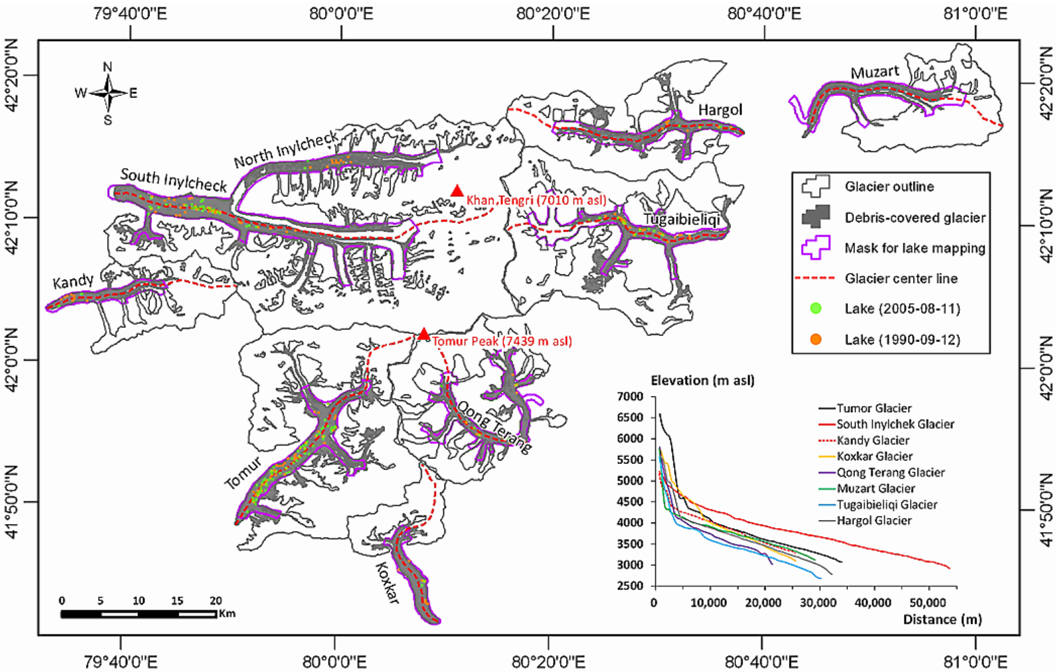

Fig. 3. Outlines of the selected glaciers (grey line), debris-covered area (grey fill) and the central flow lines (dashed red line); a shape file (purple) was used for masking the lower region of each glacier for glacial lakes mapping. The results of the 12 September 1990 and 11 August 2005 lake mapping are presented as points of lakes center; lower right inset is a plot of glacier surface profiles along the central flow lines.

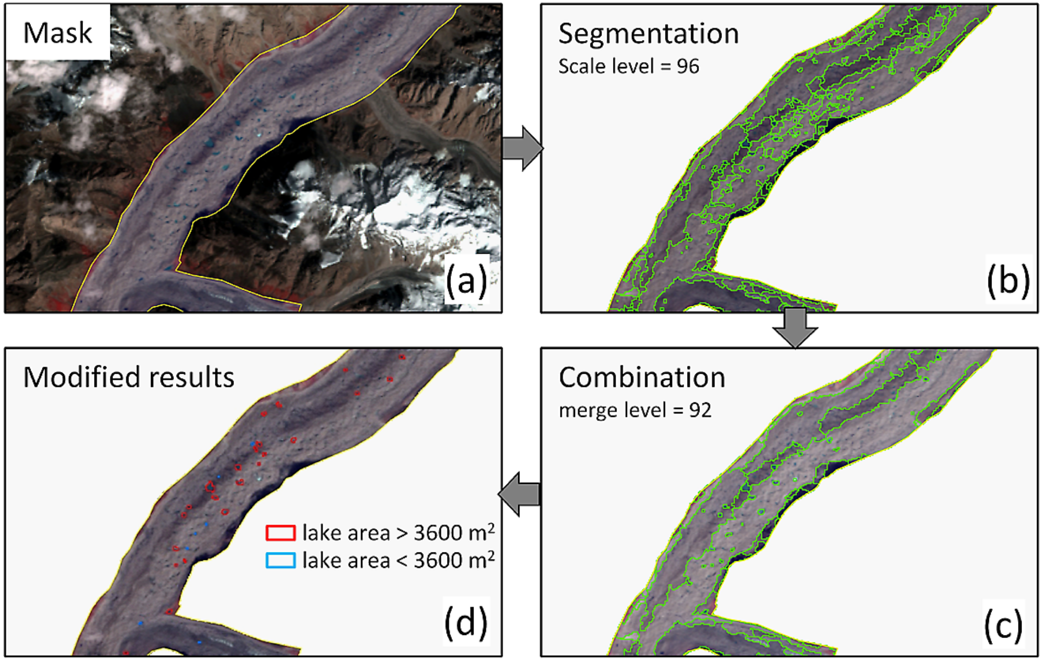

Fig. 4. Example of the supraglacial lakes mapping in the lower region of the Tomur Glacier showing the workflow of the lake extraction procedure. Background is the band combination of 432 for a Landsat TM image acquired on 24 August 2007.

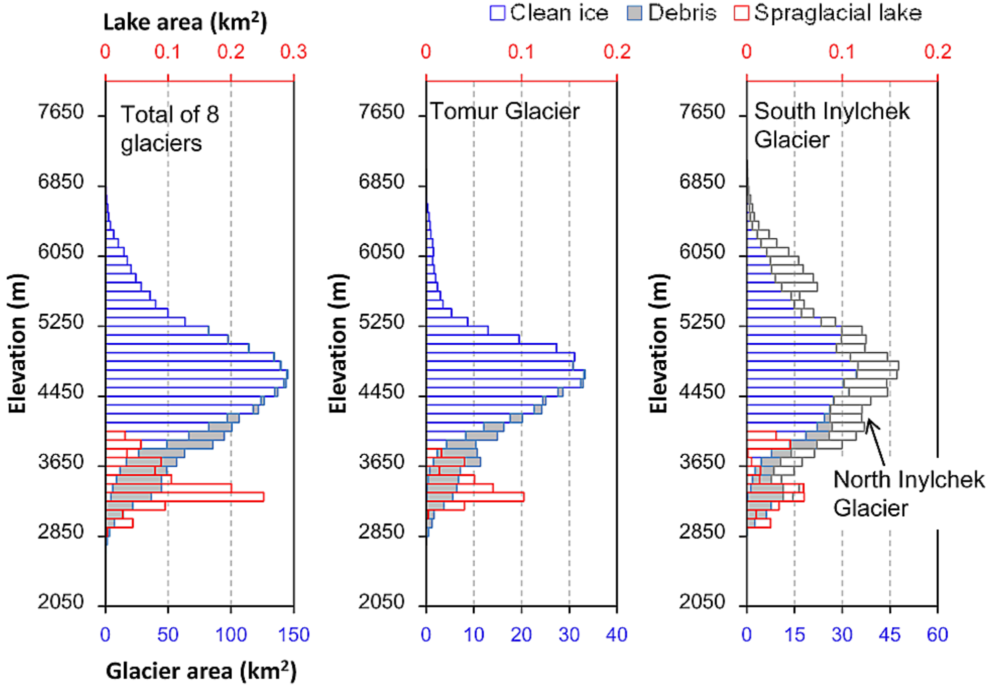

Fig. 5. Altitudinal distributions of clean ice area, debris-covered area and total supraglacial lakes area (the mean value of all years investigated) for the selected eight glaciers in the KTTM, the TG and the SIG (note the North Inylchek Glacier is also plotted for comparison).

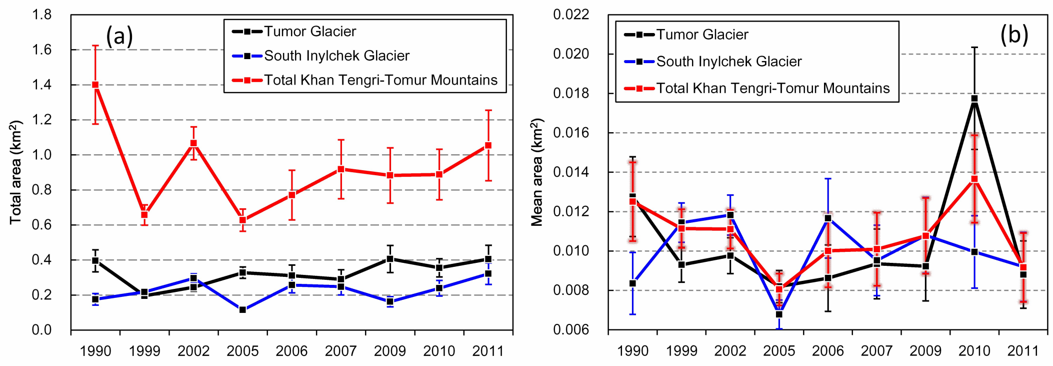

Fig. 6. Temporal variation of total **(a)** and mean **(b)** area of supraglacial lakes for the total KTTM, the TG and the SIG, between 1990 and 2011.

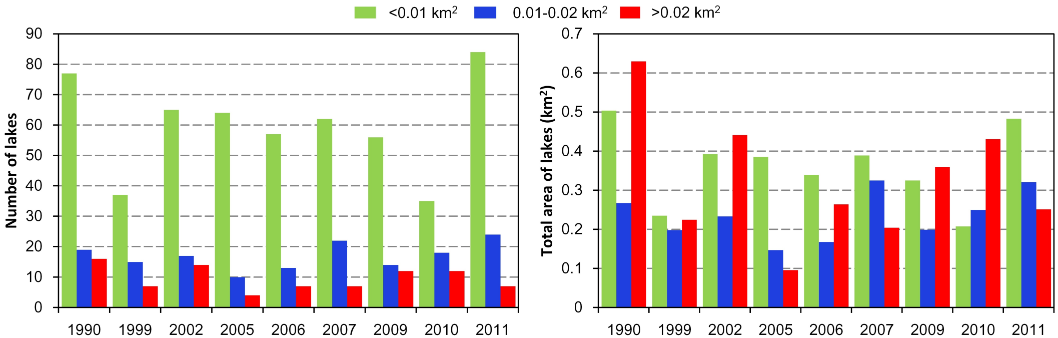

Fig. 7. Changes of numbers (left) and total area (right) for three area classes of supraglacial lakes between 1990 and 2011.

Fig. 8. A panoramic view of the lower part of Koxkar Glacier showing the wide flat ablation region covered by extensive debris cover. Photographs: Han Haidong, 12 August 2010.

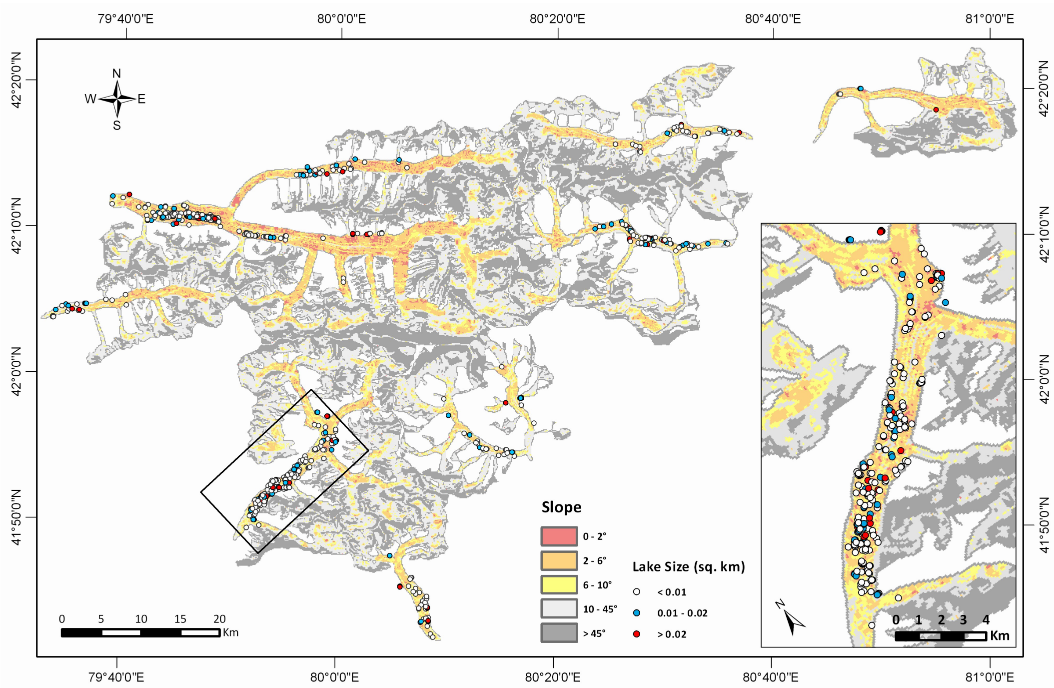

Fig. 9. Surface slope gradients of the eight glaciers in the KTTM region, overlaid by all mapped location points of lakes; inset is the detailed presentation for the lower part of the TG.

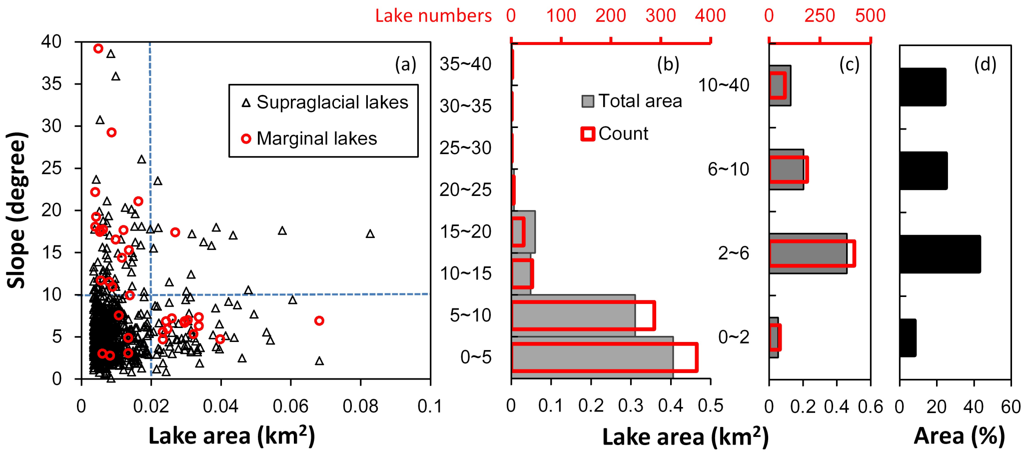

Fig. 10. **(a)**, **(b)** and **(c)** slope distributions of 775 supraglacial lakes and 38 marginal lakes mapped between 1990 and 2011 in the Khan Tengri-Tomur Mountains; **(d)** frequency distribution of the surface slope of the entire debris-covered area of the 8 glaciers.

TCD
7, 4545–4584, 2013

Fig. 11. A supraglacial lake surrounded by ice cliffs, at 3220 m a.s.l., located in the lower part of the debris-covered area of the Koxkar Glacier. Note a thin layer of debris slumping down the ice cliff and leaving many striae (people in the ellipse for scale). Photographs: Liu Qiao, on 10 August during the 2010 expedition.

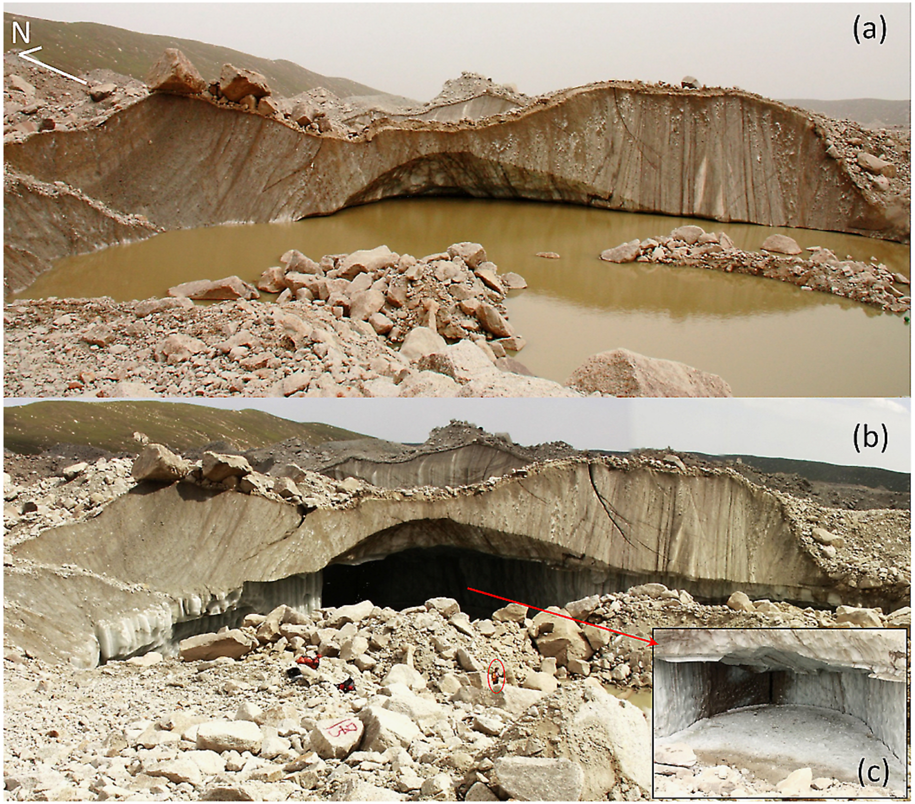

Fig. 12. A supraglacial lake, at 3235 m a.s.l., located in the middle part of the debris-covered area of the Koxkar Glacier, was visited before (**a**, 15 August 2010) and after (**b**, 19 August 2010) its drainage. Photographs: Liu Qiao and Zhang Yingsong. Note that this lake had been monitored in detail for a couple of years until the drainage (Wang et al., 2011).

TCD
7, 4545–4584, 2013

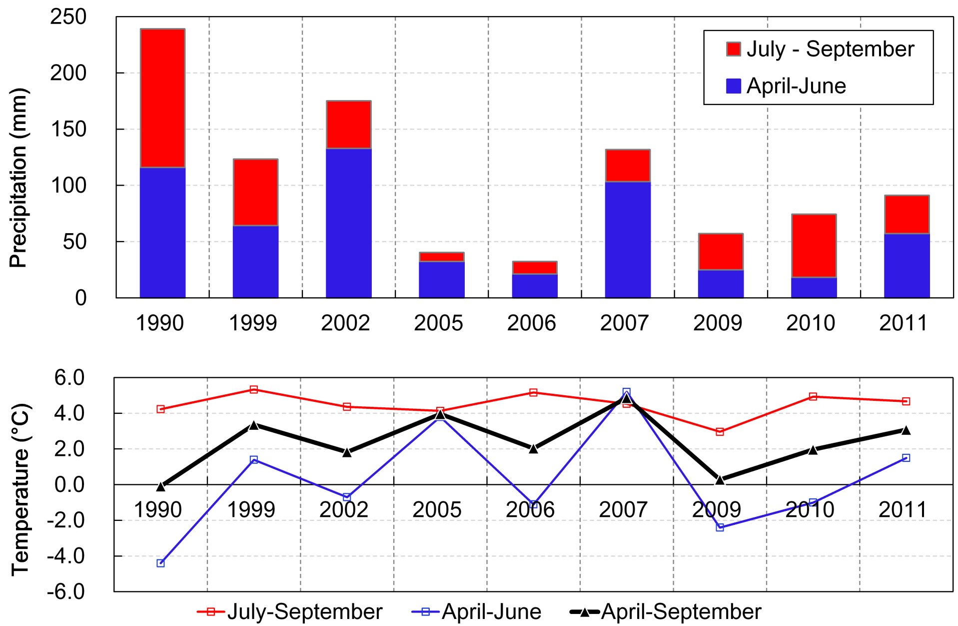

Fig. 13. Total precipitation and mean air temperature over summer (July to September) and spring (April to June) of each specific year at the Tianshan Station.

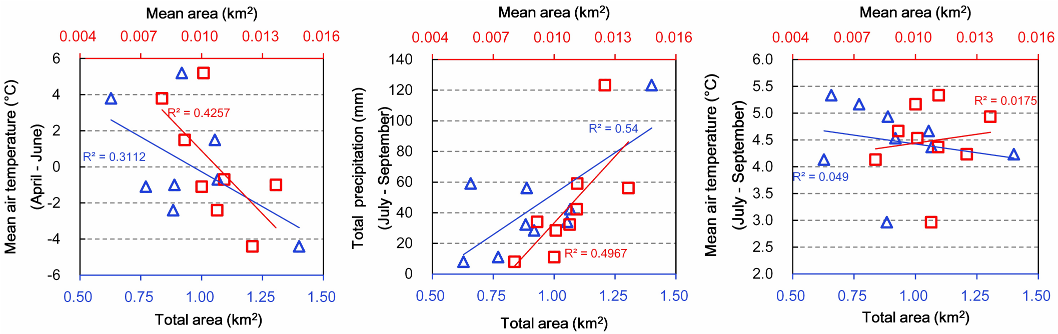

Fig. 14. Correlations between supraglacial lake area (blue triangle: total area; red square: mean area) and climatic conditions (Tianshan Station) in summer (July to September) and spring (April to June).